

## Molecular Prototypes for Spin-Based CNOT and SWAP Quantum Gates

F. Luis,<sup>1,\*</sup> A. Repollés,<sup>1</sup> M. J. Martínez-Pérez,<sup>1</sup> D. Aguilà,<sup>2</sup> O. Roubeau,<sup>1</sup> D. Zueco,<sup>1</sup> P. J. Alonso,<sup>1</sup> M. Evangelisti,<sup>1</sup>  
A. Camón,<sup>1</sup> J. Sesé,<sup>3</sup> L. A. Barrios,<sup>2</sup> and G. Aromí<sup>2,†</sup>

<sup>1</sup>*Instituto de Ciencia de Materiales de Aragón (ICMA), CSIC–Universidad de Zaragoza, and Departamento de Física de la Materia Condensada, Universidad de Zaragoza, E-50009 Zaragoza, Spain*

<sup>2</sup>*Departament de Química Inorgànica, Universitat de Barcelona, Diagonal 647, 08028, Barcelona, Spain*

<sup>3</sup>*Instituto de Nanociencia de Aragón, Universidad de Zaragoza, and Departamento de Física de la Materia Condensada, Universidad de Zaragoza, E-50018 Zaragoza, Spain*

(Received 7 March 2011; published 8 September 2011)

We show that a chemically engineered structural asymmetry in [Tb<sub>2</sub>] molecular clusters renders the two weakly coupled Tb<sup>3+</sup> spin qubits magnetically inequivalent. The magnetic energy level spectrum of these molecules meets then all conditions needed to realize a universal CNOT quantum gate. A proposal to realize a SWAP gate within the same molecule is also discussed. Electronic paramagnetic resonance experiments confirm that CNOT and SWAP transitions are not forbidden.

DOI: 10.1103/PhysRevLett.107.117203

PACS numbers: 75.50.Xx, 03.67.Lx, 75.40.Gb, 85.65.+h

Quantum computation [1,2] relies on the physical realization of quantum bits and quantum gates. The former can be in any of two distinguishable states, denoted here as spin-up  $|\uparrow\rangle$  and spin-down  $|\downarrow\rangle$ , and also, as opposed to classical bits, in any arbitrary linear superposition of these. The latter involve controlled operations on two coupled qubits [1]. The universal controlled-NOT (CNOT) gate is the archetype of such a controlled operation. It flips the target qubit depending on the state of the control qubit [see Fig. 1(a)]. This definition implies that each of the two qubits should respond inequivalently to some external stimulus, e.g., electric or magnetic fields. A SWAP gate exchanges the states of both qubits; i.e., it takes  $|\uparrow\rangle_1 \otimes |\downarrow\rangle_2$  to  $|\downarrow\rangle_1 \otimes |\uparrow\rangle_2$  and vice versa.

Solid-state candidates for these elements include superconducting circuits [3–5], spins in semiconductors [6–8], and molecular nanomagnets [9–14]. The last ones are attractive for scalability, since arrays of identical magnetic molecules can be prepared and grafted to solid substrates or devices via simple chemical methods [15,16]. The recent development of devices able to induce and readout the spin reversal of individual atoms [17–19] might also make feasible the coherent manipulation of one of these molecular qubits. State-of-the-art achievements with molecular nanomagnets include the measurement and minimization of single qubit decoherence rates [20–22] and the synthesis of mutually interacting qubit pairs [23,24]. However, the realization of a two-qubit quantum gate inside a molecular cluster remains an outstanding challenge [12,14]. Here, we show that [Tb<sub>2</sub>] molecular clusters display a magnetic asymmetry that should enable the realization of CNOT and SWAP gates.

Lanthanide ions are promising candidates for encoding quantum information [25]. For the realization of a quantum gate, it seems therefore natural to look for molecules made of just two weakly coupled lanthanide qubits. However, the

synthesis of asymmetric molecular dimers is not straightforward, as nature tends to make them symmetric. We propose a solution, sketched in Fig. 1(b), that exploits the ability of chemical design to finely tune the internal molecular structure. We synthesized a dinuclear complex of Tb<sup>3+</sup> ions, hereafter briefly referred to as [Tb<sub>2</sub>], in which the metallic dimer is wrapped by three asymmetric organic ligands [26]. Each metal ion is in a different coordination environment [see Fig. 1(c)]. In the following, we describe experiments showing that this molecular cluster fulfills the basic conditions to act as a quantum gate, namely, the appropriate definition of the two qubits, the weak coupling between them, and the magnetic asymmetry.

Measurements were performed on powdered specimens. Above 1.8 K, the ac susceptibility and magnetization were measured with a commercial SQUID magnetometer. Between 13 mK and 1.5 K, ac susceptibility data were measured with a  $\mu$ SQUID susceptometer [27], operating from 0.01 Hz up to 1 MHz. dc-magnetization measurements below 2 K were performed using a Hall microprobe installed in a dilution refrigerator. Heat capacity measurements down to  $\approx 0.35$  K were performed using the relaxation method by means of a commercial setup. Continuous-wave electronic paramagnetic resonance (EPR) experiments were carried out with a commercial setup working in the X frequency band (9.8 GHz) and under magnetic fields  $\mu_0 H \leq 1.4$  T.

The ac magnetic susceptibility  $\chi$  provides direct insight on the magnetic anisotropy of the Tb<sup>3+</sup> ions and their mutual coupling. For the lowest frequency (0.0158 Hz) and above 100 mK, the in-phase component  $\chi'$  gives the equilibrium paramagnetic response [see Fig. 2(a)]. In this regime, the cluster effective magnetic moment  $\mu_{\text{eff}} \approx (3k_B \chi' T / N_A)^{1/2}$ . At room temperature,  $\mu_{\text{eff}} = 13.7(1)\mu_B$  agrees with the effective moment of two uncoupled free ions, i.e.,  $\mu_{\text{eff}} = g_J \mu_B [2J(J+1)]^{1/2} = 13.74\mu_B$ , where

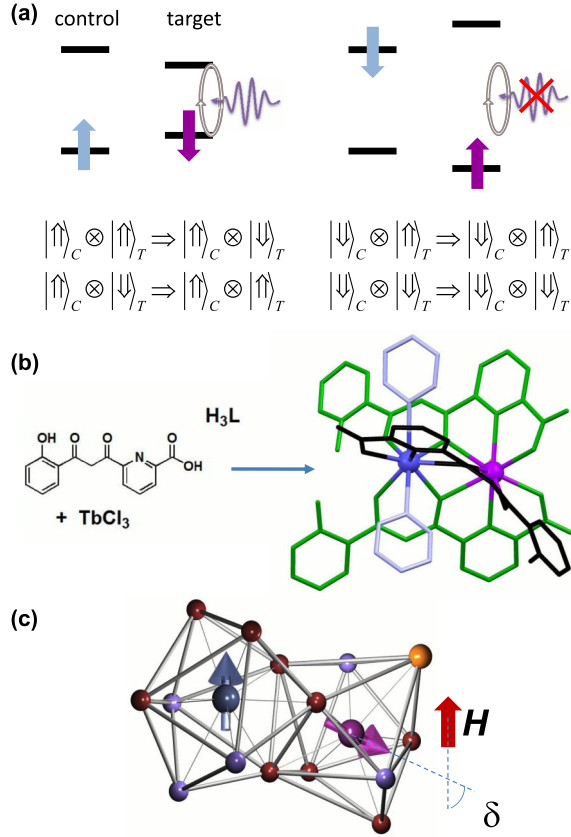


FIG. 1 (color online). (a) Illustration of a quantum CNOT operation on two coupled spin qubits. (b) Synthesis [26] of an asymmetric  $[\text{Tb}_2]$  complex using three  $\text{H}_3\text{L}$  ligands. (c) The resulting  $\text{N}_2\text{O}_6\text{Cl}$  and  $\text{N}_3\text{O}_6$  coordination polyhedra around the two  $\text{Tb}^{3+}$  ions exhibit  $C_1$  symmetry and  $C_{4v}$  symmetry, respectively [28], which induces a misalignment between their anisotropy axes: left (purple) arrow, “control”; right (blue) arrow, “target”; large light (orange) ball, Cl; small dark (red) balls, O; small light (blue) balls, N.

$g_J = 3/2$  and  $J = 6$  are the gyromagnetic ratio and the total angular momentum given by Hund’s rules. The drop observed below approximately 100 K can be assigned to the thermal depopulation of magnetic energy levels split by the crystal field. The value  $\mu_{\text{eff}} = 12.5(1)\mu_B$  measured between 3 and 10 K is close to  $\mu_{\text{eff}} = g_J\mu_B 2^{1/2}J = 12.72\mu_B$ , characteristic of two uncoupled  $\text{Tb}^{3+}$  ions whose angular momenta  $\vec{J}_1$  and  $\vec{J}_2$  point either up or down along their local anisotropy axes. The magnetic anisotropy was determined by fitting  $\chi'T$  between 3 and 300 K, using expressions derived [28,29] for the simplest uniaxial anisotropy  $\mathcal{H} = -D(J_{1,z}^2 + J_{2,z}^2)$ . The fit gives  $D/k_B = 17$  K. Excited levels are separated by more than 180 K from the ground state doublet, associated with the maximum projections  $m_J = \pm J$  [see Fig. 2(b)]. These states provide then, for each ion, a proper definition of the qubit basis  $|\uparrow\rangle \equiv |J = 6, m_J = 6\rangle$  and  $|\downarrow\rangle \equiv |J = 6, m_J = -6\rangle$ .

Below 3 K, we observe a second drop in  $\chi'T$  (Fig. 2) that we attribute to the antiferromagnetic coupling  $-2J_{\text{ex}}\vec{J}_1\vec{J}_2$

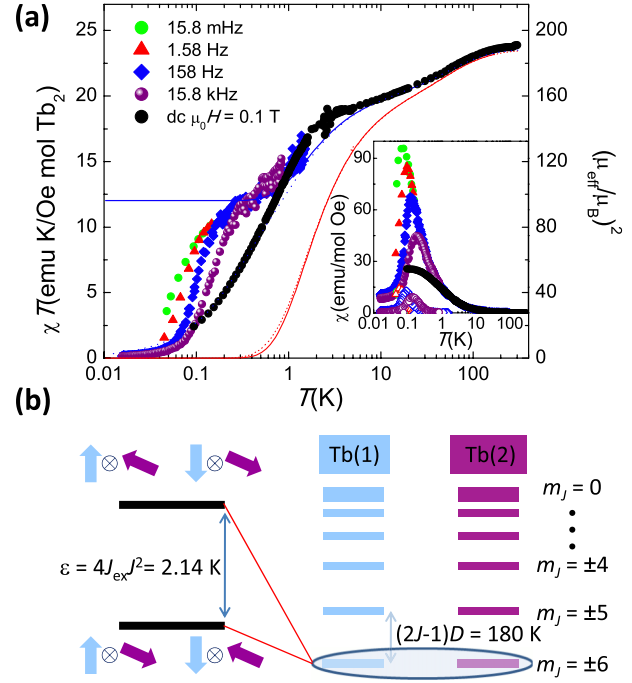


FIG. 2 (color online). (a) ac susceptibility of polycrystalline  $[\text{Tb}_2]$  at different frequencies. Main panel:  $\chi'T$  product (left axis) from which  $\mu_{\text{eff}}$  is determined (right axis). Inset:  $\chi'$  (solid symbols) and  $\chi''$  (open symbols). dc-susceptibility data measured at  $\mu_0 H = 0.1$  T are also shown. The lines are least squares fits of the ac (solid lines) and dc (dotted lines) susceptibilities for collinear ( $\delta = 0$ , red thin lines) and noncollinear ( $\delta = 66^\circ$ , blue thick lines) anisotropy axes. (b) Zero-field energy level structure of  $[\text{Tb}_2]$  derived from these fits.

of the two qubits. This interpretation is corroborated by the magnetic heat capacity  $c_{m,P}$ , shown in Fig. 3 (see [28]). At zero field,  $c_{m,P}$  shows a Schottky-type broad anomaly centered at  $T_{\text{max}} \approx 0.9$  K, which arises from the energy splitting  $\epsilon = 4J_{\text{ex}}J^2$  between antiferromagnetic ( $|\uparrow\rangle_1 \otimes |\downarrow\rangle_2$  and  $|\downarrow\rangle_1 \otimes |\uparrow\rangle_2$ ) and ferromagnetic ( $|\uparrow\rangle_1 \otimes |\uparrow\rangle_2$  and  $|\downarrow\rangle_1 \otimes |\downarrow\rangle_2$ ) states. Using the condition  $k_B T_{\text{max}} = 0.42\epsilon$ , we determine  $\epsilon/k_B \approx 2.14$  K and, from this,  $J_{\text{ex}}/k_B = -0.016(1)$  K.

Considering the value of  $\epsilon$ , the monotonic increase of  $\chi'$  down to 100 mK would be puzzling unless the magnetic moments of the two  $\text{Tb}^{3+}$  ions do not exactly compensate each other. As the coordination sphere determines the magnetic anisotropy, the easy axes of the two ions need not be parallel to each other, but can instead make a tilting angle  $\delta$ , as shown in Fig. 1. Because of this misalignment and the very strong anisotropy, even the states ( $|\uparrow\rangle_1 \otimes |\downarrow\rangle_2$  and  $|\downarrow\rangle_1 \otimes |\uparrow\rangle_2$ ) preserve a net magnetic moment. More importantly, the two ions will couple differently to an external magnetic field; i.e., their effective gyromagnetic ratios  $g_1$  and  $g_2$  will be different. For instance, if  $H$  is applied along one of the anisotropy axes, say of qubit “1,”  $g_1 = g_J$  whereas  $g_2 = g_J \cos\delta$ ; i.e., it makes the two spins inequivalent.

Susceptibility and heat capacity measurements confirm that  $g_1 \neq g_2$ . Indeed, below 10 K  $\chi'/T$  (and thus also  $\mu_{\text{eff}}$ ) is much larger than predicted for collinear anisotropy axes ( $\delta = 0$ ). In contrast, an excellent agreement is obtained for  $\delta = 66^\circ$ . We have also measured the dc susceptibility for  $\mu_0 H = 0.1$  T, obtaining further experimental evidence for noncollinear axes with the same values of  $J_{\text{ex}}$  and  $\delta$  estimated above. Heat capacity data measured under  $H \neq 0$  are shown in Fig. 3. This quantity reflects the magnetic field dependence of the energy levels, which, in its turn, should strongly depend on  $\delta$ . As with the magnetic data, the results are in qualitative and quantitative agreement with calculations made for  $\delta = 66^\circ$ .

An independent confirmation of the cluster magnetic asymmetry is given by magnetization isotherms measured at  $T = 0.26$  and 2 K, shown in Fig. 4. We find a finite paramagnetic response starting already from  $H = 0$ , which shows that the molecular ground state possesses a net magnetic moment and, therefore, that  $\delta \neq 0$  and close indeed to  $66^\circ$ . The level crossing between antiferromagnetic and ferromagnetic states gives rise to an abrupt magnetization jump, confirming the antiferromagnetic character of the exchange interactions and the value of  $J_{\text{ex}}$  determined from heat capacity experiments.

All experiments presented so far lead us to conclude that the essential physics is captured by a Hamiltonian containing the uniaxial anisotropy, the exchange couplings, the Zeeman energy, and, finally, the hyperfine interactions with the nuclear spins  $I = 3/2$  of Tb. In the reduced subspace defined by the relevant qubit states, with  $m_J = \pm 6$ , the Hamiltonian simplifies to [28]

$$\begin{aligned} \mathcal{H} = & -2J_{\text{ex}}J_{1,z}J_{2,z} - g_1\mu_B H J_{1,z} - g_2\mu_B H J_{2,z} \\ & + A_J(J_{1,z}I_{1,z} + J_{2,z}I_{2,z}), \end{aligned} \quad (1)$$

where  $A_J/k_B = 2.5 \times 10^{-2}$  K is the hyperfine constant.

Equation (1) enables us to discuss the performance of  $[\text{Tb}_2]$  as a two-qubit quantum gate. The ensuing energy level spectrum is shown in Fig. 5(b) for  $\delta = 66^\circ$ . For clarity, we show only levels with nuclear spin projections  $m_{I,1} = m_{I,2} = -3/2$ . The magnetic asymmetry enables us to univocally single out any of the desired transitions. For instance, at  $\mu_0 H = 0.07$  T, only transitions between states  $|\uparrow\rangle_1 \otimes |\downarrow\rangle_2$  and  $|\downarrow\rangle_1 \otimes |\uparrow\rangle_2$  (SWAP) would be resonant with the energy of  $\nu = 9.8$  GHz photons (X-band EPR). Notice that these two states differ in energy because  $g_1 \neq g_2$ . The fact that SWAP gate operations can be induced by electromagnetic radiation avoids the need of coherently turning on and off interactions between the two qubits that is characteristic of some existing proposals [12]. At  $\mu_0 H = 0.28$  T, the resonant transition would be that from  $|\uparrow\rangle_1 \otimes |\uparrow\rangle_2$  to  $|\uparrow\rangle_1 \otimes |\downarrow\rangle_2$  (CNOT). Therefore, SWAP and CNOT operations can be selected by tuning  $H$ . The state initialization can be easily carried out by cooling: at both fields and at  $T = 0.1$  K, the ground state population amounts to 99.3%. The short spin-lattice relaxation times ( $T_1 \simeq 4 \times 10^{-4}$  s at 0.1 K) determined from the frequency-dependent ac susceptibility data of Fig. 2 ensure that the thermal populations will be readily attained.

The realization of gate operations also requires that these transitions are allowed, e.g., by the presence of weak transverse anisotropy terms. We have checked this by performing continuous-wave EPR measurements on a  $[\text{Tb}_2]$  powdered sample. The absorption derivative measured at 6 K, shown in Fig. 5(a), consists of two broad

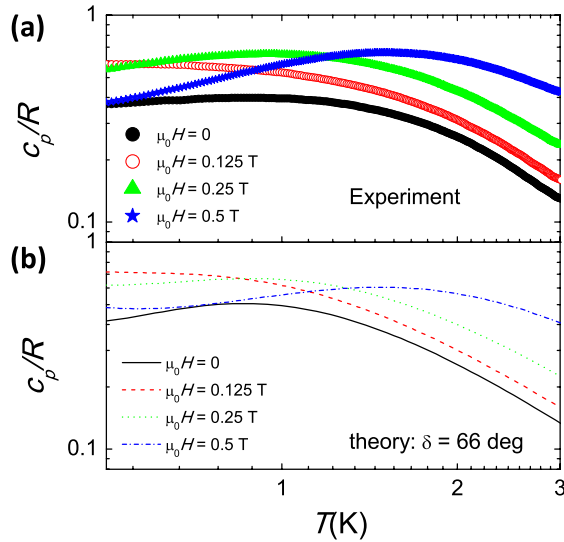


FIG. 3 (color online). (a) Magnetic heat capacity of a powdered sample of  $[\text{Tb}_2]$ . (b) Theoretical predictions for noncollinear anisotropy axes.

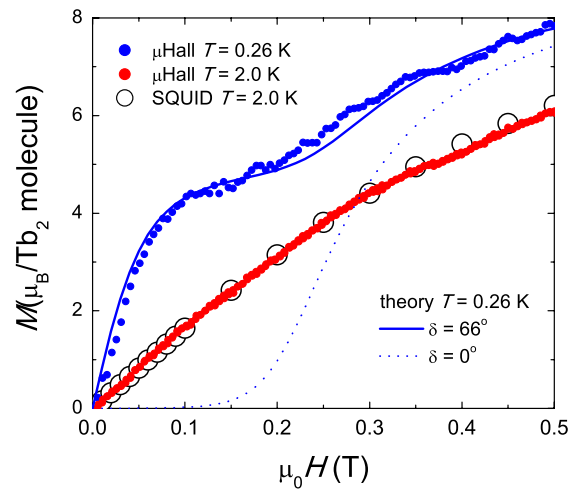


FIG. 4 (color online). Magnetization isotherms of  $[\text{Tb}_2]$ . The data at  $T = 0.26$  K are compared with calculations made for collinear ( $\delta = 0$ , dotted line) and noncollinear ( $\delta = 66^\circ$ , solid line) anisotropy axes.

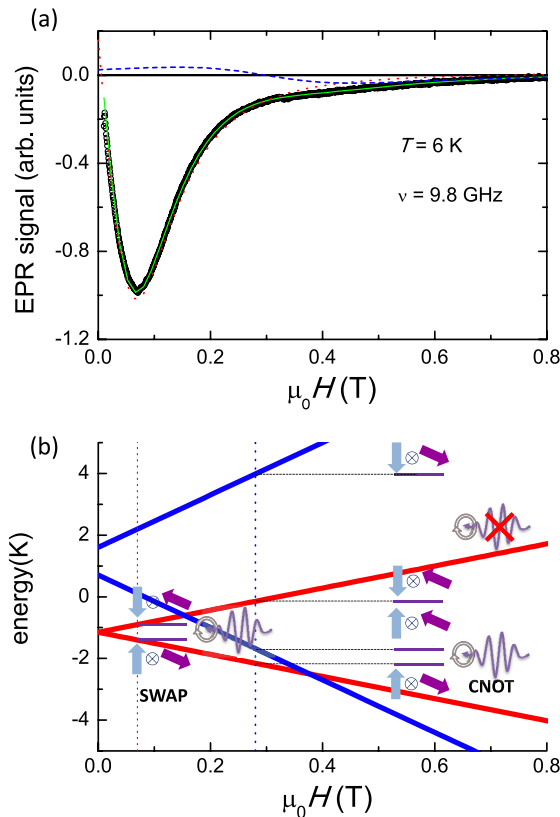


FIG. 5 (color online). (a) X-band EPR spectrum of powdered  $[\text{Tb}_2]$ . The solid line is a fit with two Lorentzian absorption contributions, shown by the dotted and dashed lines, respectively. (b) Field-dependent magnetic energy levels of  $[\text{Tb}_2]$  calculated by numerical diagonalization of Eq. (1) for  $\delta = 66^\circ$ . Only levels corresponding to magnetic nuclear states  $m_{I,1} = m_{I,2} = -3/2$  are shown.

absorption lines centered at low  $H$  and at  $\mu_0 H \approx 0.3$  T, which can be associated with the SWAP and CNOT transitions, respectively. The large widths are due to the average in orientations that is inherent to a powder measurement and also to the shift of the resonance fields depending on the nuclear spin state, as a result of the  $\Delta m_I = 0$  selection rule.

In conclusion, we have shown that molecular clusters containing two lanthanide ions meet the ingredients required to implement a CNOT quantum gate. The definition of control and target qubits is based on the magnetic inequivalence of the two ions, which has been achieved by chemically engineering dissimilar coordination spheres. The magnetic asymmetry also provides a method to realize a SWAP gate in the same cluster. Although we have only considered  $[\text{Tb}_2]$ , for which the magnetic asymmetry can be easily determined on account of its large angular momentum, the same molecular structure can be realized with other lanthanide ions [26]. This flexibility enables a vast choice of quantum gate designs. These molecular clusters are stable in solution, which opens the possibility of depositing them

onto devices able to manipulate its quantum spin state [19,30]. Chemically engineered molecular quantum gates can therefore open promising avenues for the realization of scalable quantum computing architectures.

This work was partly funded by Grants No. MAT2009-13977-C03 (MOLCHIP), No. CTQ2009-06959, FIS2008-01240, and No. FIS2009-13364-C02 from the Spanish MICINN, and the Consolider-Ingenio project on Molecular Nanoscience. Funding from the European Research Council Starting Grant FuncMolQIP (to G. A.) is also acknowledged. D.Z. acknowledges funding from ARAID foundation. G. A. acknowledges Generalitat de Catalunya for support.

\*fluis@unizar.es

†guillem.aromi@antares.qi.ub.es

- [1] M. A. Nielsen and I. L. Chuang, *Quantum Computation and Quantum Information* (Cambridge University Press, New York, 2000).
- [2] T. D. Ladd *et al.*, *Nature (London)* **464**, 45 (2010).
- [3] J. Clarke and F. K. Wilhelm, *Nature (London)* **453**, 1031 (2008).
- [4] J. H. Plantenberg, P. C. de Groot, C. J. P. M. Harmans, and J. E. Mooij, *Nature (London)* **447**, 836 (2007).
- [5] L. DiCarlo *et al.*, *Nature (London)* **460**, 240 (2009).
- [6] G. Burkard, D. Loss, and D. P. DiVincenzo, *Phys. Rev. B* **59**, 2070 (1999).
- [7] F. Jelezko, T. Gaebel, I. Popa, A. Gruber, and J. Wrachtrup, *Phys. Rev. Lett.* **92**, 076401 (2004).
- [8] R. Hanson and D. D. Awschalom, *Nature (London)* **453**, 1043 (2008).
- [9] M. Leuenberger and D. Loss, *Nature (London)* **410**, 789 (2001).
- [10] J. Tejada, E. Chudnovsky, E. del Barco, J. Hernández, and T. Spiller, *Nanotechnology* **12**, 181 (2001).
- [11] F. Troiani *et al.*, *Phys. Rev. Lett.* **94**, 207208 (2005).
- [12] J. Lehmann, A. Gaita-Ariño, E. Coronado, and D. Loss, *Nature Nanotech.* **2**, 312 (2007).
- [13] P. C. E. Stamp and A. Gaita-Ariño, *J. Mater. Chem.* **19**, 1718 (2009).
- [14] A. Ardavan and S. J. Blundell, *J. Mater. Chem.* **19**, 1754 (2009).
- [15] K. Miyake *et al.*, *J. Am. Chem. Soc.* **131**, 17808 (2009).
- [16] M. Mannini *et al.*, *Nature (London)* **468**, 417 (2010).
- [17] S. Loth, M. Etzkorn, C. P. Lutz, D. M. Eigler, and A. J. Heinrich, *Science* **329**, 1628 (2010).
- [18] A. A. Khajetoorians, J. Wiebe, B. Chilian, and R. Wiesendanger, *Science* **332**, 1062 (2011).
- [19] M. Urdampilleta, S. Klyatskaya, J.-P. Cleuziou, M. Ruben, and W. Wernsdorfer, *Nature Mater.* **10**, 502 (2011).
- [20] A. Ardavan *et al.*, *Phys. Rev. Lett.* **98**, 057201 (2007).
- [21] S. Bertaina *et al.*, *Nature (London)* **453**, 203 (2008).
- [22] C. Schlegel, J. van Slageren, M. Manoli, E. K. Brechin, and M. Dressel, *Phys. Rev. Lett.* **101**, 147203 (2008).
- [23] G. A. Timco *et al.*, *Nature Nanotech.* **4**, 173 (2009).
- [24] A. Candini *et al.*, *Phys. Rev. Lett.* **104**, 037203 (2010).
- [25] S. Bertaina *et al.*, *Nature Nanotech.* **2**, 39 (2007).
- [26] D. Aguilà *et al.*, *Inorg. Chem.* **49**, 6784 (2010).

- [27] M. J. Martínez-Pérez, J. Sesé, F. Luis, D. Drung, and T. Schurig, *Rev. Sci. Instrum.* **81**, 016108 (2010).
- [28] See Supplemental Material at <http://link.aps.org/supplemental/10.1103/PhysRevLett.107.117203> for further details on the structural and physical characterization of the samples, as well as for a theoretical derivation of Eq. (1).
- [29] J. L. Garcia-Palacios, J. B. Gong, and F. Luis, *J. Phys. Condens. Matter* **21**, 456006 (2009).
- [30] A. Imamoglu, *Phys. Rev. Lett.* **102**, 083602 (2009).